A post-HF approach to the Sunscreen Octyl Methoxycinnamate

Ettore Fois,[1] Mario Oriani,[1] and Gloria Tabacchi[1, a)]

Department of Science and High Technology, University of Insubria and INSTM UdR Insubria
Via Valleggio 11, I-22100 Como (Italy)

(Dated: 31 January, 2021)

Octyl methoxycinnamate (OMC) is a commercial sunscreen with excellent UVB filter properties. However, it is known to undergo a series of photodegradation processes that decrease its effectiveness as UVB filter. In particular, the trans (E) form - which is considered so far the most stable isomer - converts to the cis (Z) form under the effect of light. In this work, by using post-Hartree-Fock approaches (CCSD, CCSD(t) and CCSD+T(CCSD)) on ground state OMC geometries optimized at the MP2 level we show that the cis and trans form of the gas-phase OMC molecule have comparable stability. Our results suggest that the cis form is stabilized by intra-molecular dispersion interactions, leading to a folded, more compact structure than the trans isomer.

---

a) Electronic mail: gloria.tabacchi@uninsubria.it

I. INTRODUCTION

The sunburn risk by UV has long been recognized: typically UVB radiation (315 nm – 280 nm) induces erythema and direct DNA damage, while the deleterious consequence on human skin of UVA radiation (400 nm - 315 nm) include, among others, DNA mutation and collagen degradations.[1] The use of sunscreen products containing molecular UV filters is fundamental to prevent these harmful effects.[2]

Octil methoxycinnammate (OMC) also known as 2-ethylhexyl 4-methoxycinnamate, or by its commercial name octinoxate, is a widely used UVB filter in sunscreen products because it does not stain and does not cause skin irritation.[2,3] In spite of its proven efficacy in UVB protection, various studies demonstrated that trans-octinoxate is unstable upon exposure to light, both in solution and in sunscreen lotions, leading to a decrease in photoprotection.[4–19]. Experiments conducted on sunscreen products indicated the predominance of octinoxate photolysis over photoisomerization due to interactions with other filters in the formulation[11,20,21]. On the other hand, in the absence of other sunscreen agents, the trans-cis isomerization has been recognized as the prevailing photodegradation mechanism of octinoxate, both in protic solvents (methanol, water) and in apolar media such as cyclohexane[13,14]. Both octinoxate isomers have very close maximum absorption wavelenghts (about 290 nm in cyclohexane and around 310 nm in protic solvents).[4,9–16,19]. However, the cis form has a lower absorption capacity than the trans isomer, hence a lower efficacy as a UVB filter.[2,10,13,14]

More recently, experimental techniques such as ultrafast transient absorption spectroscopy,[22,23] both in the gas phase and in microsolvation environments, have been adopted for evaluating the fate of cinnamate-based organic filters under UV irradiation[24–26]. In particular, Tan et al.[27], by employing resonance two-photon ionization (R2PI), examined the photorelaxation behaviour of trans-octinoxate as isolated molecules in the gas phase and in microsolvation water environment. They ascribed the measured nanosecond-scale lifetimes in the gas phase to a long-lived $^{1}1n\pi^{*}$ state. Subsequent studies on other cinnamate derivatives evidenced that such a $^{1}1n\pi^{*}$ state becomes destabilized in the presence of water, with a decrease of the relaxation lifetime to the order of ps.[28,29] Peperstraete et al., by using time-resolved pump–probe spectroscopy, highlighted for gas-phase octinoxate a non-radiative decay from $^{1}1\pi\pi^{*}$ to the $^{1}1n\pi^{*}$ state and a subsequent deexcitation to the electronic graund state S_0.[30] On the other hand, in solution environments (cyclohexhane and ethanol) the trans–cis isomerization process becomes of greater relevance for the photochemistry of this molecule.[30] Very recently, Muramatsu et al.[31] adopted Resonant Two-foton Ionization (R2PI) and Laser-Induced-Fluorescence (LIF) to study the electronic spectrum of jet-cooled trans-octinoxate. Using the UV/UV hole-burning technique and Density Functional Theory (DFT) calculations, these authors reported the existence of at least three isomers, which should be responsible of the broad feature observed in the R2PI spectra of jet-cooled octinoxate.[27,31]

In this context, a number of theoretical studies have investigated with a variety of techniques, including high-level quantum chemical approaches (complete active space self-consistent field (CASSCF) and multi-state complete active space 2nd-order perturbation (MS-CASPT2)), the photophysical and photochemical properties of several cinnamate derivatives and/or reduced models of OMC - namely molecular structures including only the cinnammate chromophore nucleus but not the long alifatic chain.[32–43]. For example, the trans-cis photoisomerization route of substituted methylcinnamates was recently explored via single-component artificial force-induced reaction (SC-AFIR) combined with time-dependent density functional theory (TD-DFT), highlighting a marked influence of the phenyl substituents on the decay mechanism[42]. Other studies at the TD-DFT/CIS level suggested appreciable solvent and hydrogen-bond effects on the photoisomerization mechanisms,[28,29] which were then corroborated by CASSCF and MS-CASPT2 calculations[37,44]. Overall, these researches on cinnamates basically agree on indicating C=C bond twisting as the dominant reaction coordinate leading to a conical intersection, after which the molecule can either reconvert to the trans-form or evolve to the cis-isomer.[28,37,42,45,46] Nonetheless, the nature of the molecule - in particular, the presence of phenil ring substituents - may affect the relaxation dynamics in the excited states leading to different ratios of cis vs. trans-isomers.[42,46] Also interestingly, whereas the photochemistry of the trans form of these cinnamate derivatives has been widely studied, less attention has been dedicated to the cis isomer - one exception being the model plant sunscreen methyl-[41] and ethyl-[47] sinapates, where the efficiency of photoprotection has been found to be independent of the trans or cis form.[47]

On a different note, other computational investigations, were mostly devoted to the exploration of the stability of plausible isomers of the entire OMC molecule, and performed at the DFT level[31,35,48–51]. Indeed, a large number of conformational isomers can exist, due to the possible rotations of the propenyl single bond and the seven C-C bonds of the aliphatic chain. Overall, the latter studies indicated the predominant stability of the trans-OMC form over the cis-OMC form - in particular, an energy difference of 4.7 kcal/mol in favour of the trans isomer was calculated at the B3LYP/6-311++G(d,p) level[50]. Regarding the trans-OMC, also a theoretical study of many

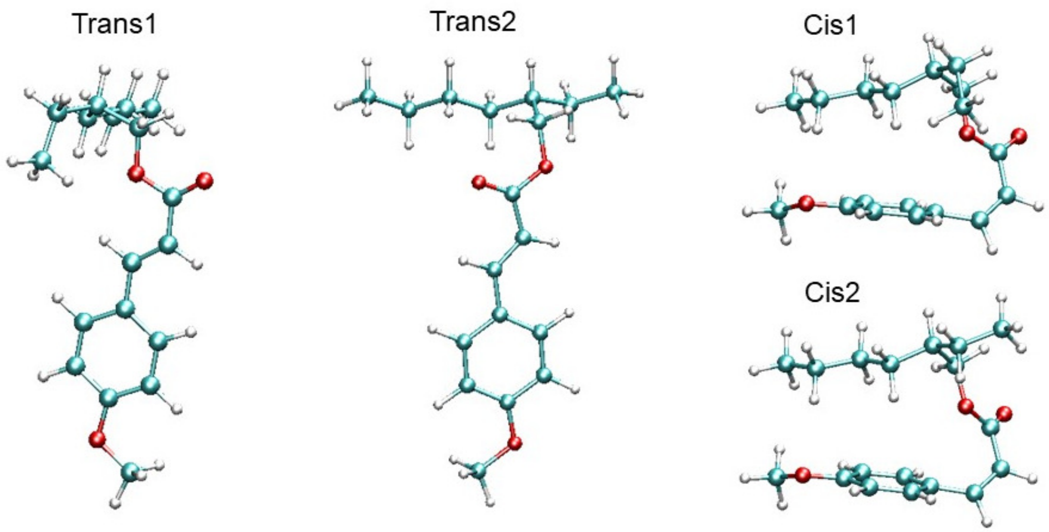

FIG. 1. Graphical representation of the mp2/cc-pvdz+S optimized structures of the four selected OMC conformers. Atom color codes: O=red; C=cyan; H=white.

possible conformers has been performed at the DFT-lavel, indicating that several of these conformers are thermally accessible at ambient conditions,[31] in line with the broad spectral patterns experimentally obtained.[27,31]

In this scenario, to the best of our knowledge, an investigation of the relative stability of cis- vs. trans- octinoxate beyond the DFT level of theory is still missing. Herein, we present a study based on post-Hartree-Fock (post-HF) calculations of different groud-state OMC forms, including two cis- (Z) and two trans- (E) isomers. Because of the huge number of possible conformers due to single-bond rotation, rather than focusing on the search of the most stable conformer, our investigation is targeted at identifying, using correlated wavefunction methods, the leading features responsible of the trans vs cis stabilization.

II. COMPUTATIONAL DETAILS

A first guess structure for the trans-OMC conformer (Trans1) was obtained by annealing a first principles molecular dynamics (FPMD)[52] trajectory (using the PBE-D2 functional[53,54]) from 300 K to 0 K in the gas phase. The structure of the second trans- conformer (Trans2) was taken from the literature - namely, the lowest-energy trans-conformer as reported in Ref.[31], which was

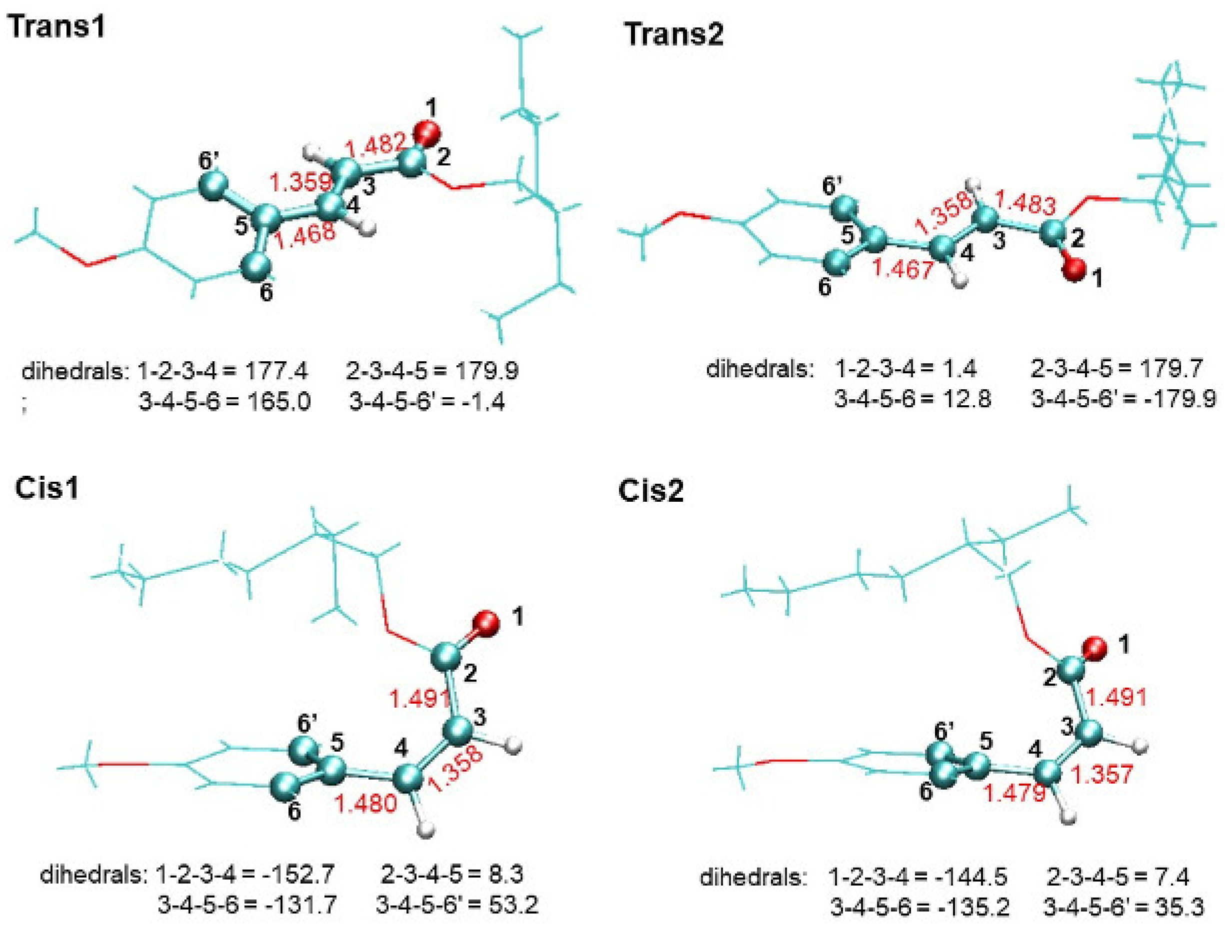

FIG. 2. Graphical representation of the four mp2/cc-pvdz+S optimized structures of OMC. Atoms relevant for π conjugation are represented as ball-and-sticks, while the others are represented as lines (color codes as in Fig.1). Angles in degrees, distances in Å.

obtained at the ωb97xd/6-311g(d,p) level.[31]

As regards the cis forms of OMC, two cis-conformers (Cis1 and Cis2) were selected in the same way as the Trans1 conformer, by annealing two different FPMD trajectories from 300 K to 0 K.

The geometries of the chosen cis- and trans- OMC conformers were then optimized at the mp2[55] level of theory using the cc-pvdz basis set augmented by diffuse s-functions for all atoms (mp2/cc-pvdz+S). Also, normal modes analysis was performed at this level of theory in order to obtain zero-point-energies (zpe). All frequencies were positive, thus the geometries were true minima in the potential energy surfaces. Adopting these optimized structures, single point mp2 energies (see Table I) were obtained by using larger basis set, namely the Dunning-Hay full-double-ζ

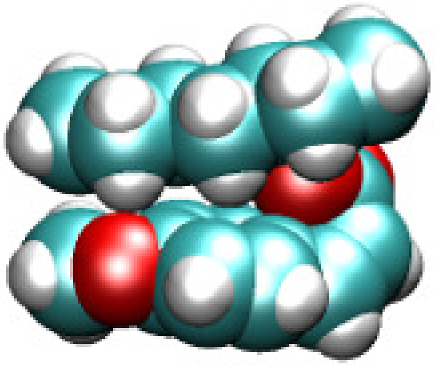

FIG. 3. van-der-Waals representation of the Cis2 isomer optimized at the mp2/cc-pvdz+S level. Atom color codes as in Fig.1.

plus polarization plus diffuse dzp++[56], the correlation-consistent basis sets aug-cc-pvdz and aug-cc-pvtz,[57] the triple-ζ plus polarization (tzp) and plus diffuse (tzp++).[58,59] Table I comprises also the zpe-corrected Hartree-Fock (HF) single-point energies calculated on the same geometries with the cc-pvdz+S and tzp++ basis set.

Moreover, single point energies of the four conformers were also calculated by adopting different Coupled-Clusters (CC)[60,61] approaches, namely the CCSD[62], CCSD(t),[63] and the CCSD-T(CCSD)[64] approximations. In these cases, two different double-ζ basis set were used: the cc-pvdz-S one[57], and a full double-ζ plus polarization and diffuse functions (dzp++). Zpe-corrected CC energies are reported in Table II. The Frozen Core approximation was adopted throughout, with the only exception of the tzp++ basis set.

The FPMD runs for the guess structures were performed using the CPMD code[52,65,66], adopting ultra-soft pseudopotentials at 30 Ry cutoff of the wavefunctions expansion with planewave basis set, while the rest of the adopted FPMD protocol was as in Refs.[67–71]. The geometry optimization and mp2 calculations on the guess structures were performed with the Gaussian09[72] code, while all the CC calculations were performed with the NWCHEM[73,74] code. Basis sets were available either from Gaussian09/NWCHEM or from the Basis Set Exchange library at basissetexchange.org[75].

III. RESULTS AND DISCUSSION

The four optimized structures, depicted in Figure 1, suggest the leitmotiv underlining the relative stability of the cis- vs trans- forms of OMC. In the trans-OMC structures, the extension of the π conjugation seems to be the stabilizing and structure-determining driving force. On the other hand, in the cis-OMC's the van-der-Waals like interaction (vdw) between the cinnamate backbone and the aliphatic chain appears to be the structure-determining driving force.

Interestingly, the two kinds of interaction, the π-conjugation vs vdw, seem to be reciprocally self-excluding. The relevant dihedral angles involving the Z or E C-C double bond are reported in Figure 2. In the cis isomers, these angles clearly indicate large distortions of the cinnamate backbone from the ideal planar structure, which would be functional to a stabilizing π-conjugation. Conversely, in the trans- forms, the cinnamate out-of-plane distortion is quite modest. However, the E arrangement of the C3-C4 double bond (see Figure 2) does not allow for the intra-molecular vdw stabilizing interaction envisaged in the cis-OMC structures. Besides the dihedral angles values - that highlight a more planar conjugate backbone - also the C4-C5 distances, which are shorter in both trans conformers, indicate that the trans conformers have a more extended π structure than the cis ones.

Actually, the challenging issue of whether intra-molecular vdw interactions might compete with extended π conjugation is offered by the cis- vs trans- OMC relative stability. Importantly, such an issue has practical relevance as well, because both trans-to-cis and cis-to-trans light-induced isomerizations are supposed to occur in commercial OMC-based sunscreen products.

Let us now discuss the energetics of the studied OMC conformers. First of all, we notice that the zpe is higher for the cis isomers, suggesting that the trans forms might be slightly favoured. Actually, this occurs at the mp2/cc-pvdz+S level, where the Cis2 electronic energy (-924.4519260 Hartree) is lower than the corresponding value for the Trans2 conformer (-924.4514416 Hartree) - amounting to an electronic energy difference of -0.304 kcal/mol in favor of Cis2. Interestingly, at the same level of theory, the zpe contribution also reverts the stability order of the Cis1 and Trans1 forms - namely, the Cis1 vs Trans1 electronic energy difference is -0.915 kcal/mol in favour of Cis1. These results may appear unexpected, as, in the previous literature, on the basis of hybrid-DFT calculations, OMC trans isomers (with respect to the C3=C4 double bond) are quoted to be more stable than the cis ones in both gas and solution phases .[48,50,76]

On the other hand, the higher stability of Trans2 with respect to Trans1 is not surprising, as the

Trans2 geometry had been obtained from an accurate conformational analysis refined at the DFT level, including both approximated dispersion and zpe corrections.[31] Indeed, the Trans2 structure is characterized by a very good planarity, as also evidenced by the dihedral angles and by the C4-C5 bond lenght, suggesting a stronger degreee of π delocalizzation betweeen the cinnamate phenyl ring and the (E)-C3=C4 double bond (see Figure 2). As regards the energetics of the two cis structures, a possible explanation of the greater stability of Cis2 *vs* Cis1 is the nearly-linear zig-zag arrangement of the alkyl chain, along with the higher extent of π conyugation as denoted by the slightly shorter C4-C5 bond lenght.

The data reported in Tables I and II indicate that the above discussed greater relative stability of Trans2 with respect to Trans1 and of Cis2 with respect to Cis1 is mainthained throughout all the correlated wavefunction method/basis set combinations investigated in this work.

A closer inspection of Tables I and II reveals a strong dependence of the cis-vs-trans relative stability from both basis set and level of theory. At the mp2 level, the larger triple-ζ basis set favours the Trans2 isomer. However, by releasing the frozen core approximation at the atzp++ level, the Cis2 structure becomes more stable than Trans2. Notably, the Cis2 isomer is also favoured at the CCSD+T(CCSD)/dzp++ level of theory (Table II).

An interesting point emerges by inspecting the CC/dzp++ energies trend (Table II): the Trans2 is favoured at the CCSD level, while, by including triples, the situation is reversed and the Cis2 is predicted as the most stable structure. It should be stressed, however, that the energy differences between the two most stable isomers (Cis2 and Trans2) with the larger basis set (dzp++, see Table II) are always within the kcal/mol. In particular, such energy differences are nearly equal to kT (at 298 K) at the CCSD+T(CCSD)/dzp++ level. In addition, the energy difference between the two most stable isomers (Cis2 and Trans2) calculated at the mp2 level with the largest basis set (tzp++, see Table I), is below 1 kcal/mol with the Frozen Core approximation, and it becomes lower than kT (at 298 K) by including full-core correlation.

Notably, the cis-trans energy differences predicted at the HF level (Table I) are larger than 10 kcal/mol, indicating that dispersion interactions are playing a substantial role in stabilizing the cis structures by favouring folded geometries characterized by significant intra-molecular vdw interactions between the aliphatic and π structures, as shown in Figure 3 for the Cis2 conformer. Such a folding, which should likely accompany the trans-cis OMC isomerization, brings about substanzial size changes in the molecular shape. These structural changes can be quantitatively estimated by inspecting Table III, where the Inertia moments of the four investigated conformers are reported. Indeed, the inertia moments along two principal axes nearly double in passing from the cis1/cis2 to the trans1/trans2 isomers, leading to a quite different rotational behaviour of the two isomers. This finding might be a clue for explaining the efficient non-radiative heat transfer experimentally associated to the trans-cis interconversion[30,31].

IV. CONCLUSIONS

In this work we have presented a computational analysis on the relative stability of cis-OMC vs trans-OMC, a molecule largely used as component of UV-protecting sunscreen creams. Adopting post-HF level calculations up to the CCSD-T(CCSD) level of theory we could predict that the cis-OMC isomer could be more stable than previously reported, and that its ground state energy is slightly lower than the energy of trans-OMC. We could moreover pinpoint the reason of such a greater stability: in the cis conformers, the two structural motifs of the molecule - a nearly linear aliphatic chain and a cinnamate backbone - may interact favourably via van der Waals interactions. This interaction is strong enough to match the loss of π-conjugation as a consequence of folding. On the other hand, the stability of the trans conformers is likely due to a large π-conjugations, while the trans (E) arrangement hinders the folding needed to achieve maximum intra-molecular van der Waals stabilization. With respect to the practical use of OMC as UV filter, the most accurate analyses indicate a co-partecipation of both isomers to the filtering effects: the trans-OMC (which has a larger π-conjugation) absorbs light in the 300 nm region. Then, it converts to cis-OMC (a poorer absorber), which non-radiatively releases heat to the ambient. We might argue that in the trans(unfolded)-to-cis(folded) light-induced conversion, the variation of molecular size (thus, the change in the inertia moments) here highlighted might effectively contribute to the dissipation of the energy accumulated upon light absorption. In perspective, the behaviour, at thermal energy, of the two isomers could be in principle investigated via molecular dynamics simulations to fully capture the differences in their complex rotational characteristics.

V. DEDICATION

This paper honors Giorgina Corongiu for her pioneering contributions to quantum chemistry.

ACKNOWLEDGMENTS

Financial support of University of Insubria FAR2019 is gratefully acknowledged. Dr. Cristiano Invernizzi is gratefully acknowledged for useful discussions.

REFERENCES

[1] T. Diepgen and V. Mahler, "The epidemiology of skin cancer," British Journal of Dermatology **146**, 1–6 (2002).

[2] N. A. Shaath, "Ultraviolet filters," Photochemical and Photobiological Sciences **9**, 464–469 (2010).

[3] D. R. Sambandan and D. Ratner, "Sunscreens: An overview and update," Journal of the American Academy of Dermatology **64**, 748–758 (2011).

[4] S. Pattanaargson and P. Limphong, "Stability of octyl methoxycinnamate and identification of its photo-degradation product," International Journal of Cosmetic Science **23**, 153–160 (2001).

[5] H. Gonzenbach, T. J. Hill, and T. G. Truscott, "The triplet energy levels of uva and uvb sunscreens," Journal of Photochemistry and Photobiology, B: Biology **16**, 377–379 (1992).

[6] J. K. Broadbent, B. S. Martincigh, M. W. Raynor, L. F. Salter, R. Moulder, P. Sjöberg, and K. E. Markides, "Capillary supercritical fluid chromatography combined with atmospheric pressure chemical ionisation mass spectrometry for the investigation of photoproduct formation in the sunscreen absorber 2-ethylhexyl-p-methoxycinnamate," Journal of Chromatography A **732**, 101–110 (1996).

[7] V. Ambrogi, L. Latterini, F. Marmottini, C. Pagano, and M. Ricci, "Mesoporous silicate mcm-41 as a particulate carrier for octyl methoxycinnamate: Sunscreen release and photostability," Journal of Pharmaceutical Sciences **102**, 1468–1475 (2013).

[8] O. I. Parisi, D. Aiello, M. F. Casula, F. Puoci, R. Malivindi, L. Scrivano, and F. Testa, "Mesoporous nanocrystalline tio2 loaded with ferulic acid for sunscreen and photo-protection: Safety and efficacy assessment," RSC Advances **6**, 83767–83775 (2016).

[9] N. Serpone, A. Salinaro, A. V. Emeline, S. Horikoshi, H. Hidaka, and J. Zhao, "An in vitro systematic spectroscopic examination of the photostabilities of a random set of commercial sunscreen lotions and their chemical uvb/uva active agents," Photochem. Photobiol. Sci. **1**, 970–981 (2002).

[10]S. Pattanaargson, T. Munhapol, P. Hirunsupachot, and P. Luangthongaram, "Photoisomerization of octyl methoxycinnamate," Journal of Photochemistry and Photobiology A: Chemistry **161**, 269–274 (2004).

[11]R. M. Sayre, J. C. Dowdy, A. J. Gerwig, W. J. Shields, and R. V. Lloyd, "Unexpected photolysis of the sunscreen octinoxate in the presence of the sunscreen avobenzone¶," Photochemistry and Photobiology **81**, 452 (2005).

[12]L. A. MacManus-Spencer, M. L. Tse, J. L. Klein, and A. E. Kracunas, "Aqueous photolysis of the organic ultraviolet filter chemical octyl methoxycinnamate," Environmental Science and Technology **45**, 3931–3937 (2011).

[13]S. P. Huong, V. Andrieu, J. P. Reynier, E. Rocher, and J. D. Fourneron, "The photoisomerization of the sunscreen ethylhexyl p-methoxy cinnamate and its influence on the sun protection factor," Journal of Photochemistry and Photobiology A: Chemistry **186**, 65–70 (2007).

[14]K. M. Hanson, S. Narayanan, V. M. Nichols, and C. J. Bardeen, "Photochemical degradation of the uv filter octyl methoxycinnamate in solution and in aggregates," Photochemical and Photobiological Sciences **14**, 1607–1616 (2015).

[15]T. M. Karpkird, S. Wanichweacharungruang, and B. Albinsson, "Photophysical characterization of cinnamates," Photochemical and Photobiological Sciences **8**, 1455–1460 (2009).

[16]A. J. M. Santos, M. S. Miranda, and J. C. E. da Silva, "The degradation products of uv filters in aqueous and chlorinated aqueous solutions," Water Research **46**, 3167–3176 (2012).

[17]C. Puglia, F. Bonina, L. Rizza, P. Blasi, A. Schoubben, R. Perrotta, M. S. Tarico, and E. Damiani, "Lipid nanoparticles as carrier for octyl-methoxycinnamate: In vitro percutaneous absorption and photostability studies," Journal of Pharmaceutical Sciences **101**, 301–311 (2012).

[18]A. L. M. Daneluti, F. M. Neto, M. V. R. Velasco, A. R. Baby, and J. do Rosário Matos, "Evaluation and characterization of the encapsulation/entrapping process of octyl methoxycinnamate in ordered mesoporous silica type sba-15," Journal of Thermal Analysis and Calorimetry **131**, 789–798 (2018).

[19]R. Rodil, M. Moeder, R. Altenburger, and M. Schmitt-Jansen, "Photostability and phytotoxicity of selected sunscreen agents and their degradation mixtures in water," Analytical and Bioanalytical Chemistry **395**, 1513–1524 (2009).

[20]D. Dondi, A. Albini, and N. Serpone, "Interactions between different solar uvb/uva filters contained in commercial suncreams and consequent loss of uv protection," Photochemical and Photobiological Sciences **5**, 835–843 (2006).

[21] S. Scalia and M. Mezzena, “Photostabilization effect of quercetin on the uv filter combination, butyl methoxydibenzoylmethane-octyl methoxycinnamate,” Photochemistry and Photobiology **86**, 273–278 (2010).

[22] L. A. Baker, S. E. Greenough, and V. G. Stavros, “A perspective on the ultrafast photochemistry of solution-phase sunscreen molecules,” Journal of Physical Chemistry Letters **7**, 4655–4665 (2016).

[23] E. L. Holt and V. G. Stavros, “Applications of ultrafast spectroscopy to sunscreen development, from first principles to complex mixtures,” International Reviews in Physical Chemistry **38**, 243–285 (2019).

[24] K. M. Krokidi, M. A. P. Turner, P. A. J. Pearcy, and V. G. Stavros, “A systematic approach to methyl cinnamate photodynamics,” Molecular Physics **119**, e1811910 (2021).

[25] J. M. Woolley, R. Losantos, D. Sampedro, and V. G. Stavros, “Computational and experimental characterization of novel ultraviolet filters,” Physical Chemistry Chemical Physics **22**, 25390–25395 (2020).

[26] S. Kenjo, Y. Iida, N. Chaki, S. nosuke Kinoshita, Y. Inokuchi, K. Yamazaki, and T. Ebata, “Laser spectroscopic study on sinapic acid and its hydrated complex in a cold gas phase molecular beam,” Chemical Physics **515**, 381–386 (2018).

[27] E. M. Tan, M. Hilbers, and W. J. Buma, “Excited-state dynamics of isolated and microsolvated cinnamate-based uv-b sunscreens,” Journal of Physical Chemistry Letters **5**, 2464–2468 (2014).

[28] Y. Miyazaki, K. Yamamoto, J. Aoki, T. Ikeda, Y. Inokuchi, M. Ehara, and T. Ebata, “Experimental and theoretical study on the excited-state dynamics of ortho-,meta-, and para-methoxy methylcinnamate,” Journal of Chemical Physics **141**, 244313 (2014).

[29] Y. Miyazaki, Y. Inokuchi, N. Akai, and T. Ebata, “Direct spectroscopic evidence of photoisomerization in para -methoxy methylcinnamate revealed by low-temperature matrix-isolation ftir spectroscopy,” Journal of Physical Chemistry Letters **6**, 1134–1139 (2015).

[30] Y. Peperstraete, M. Staniforth, L. A. Baker, N. D. Rodrigues, N. C. Cole-Filipiak, W. D. Quan, and V. G. Stavros, “Bottom-up excited state dynamics of two cinnamate-based sunscreen filter molecules,” Physical Chemistry Chemical Physics **18**, 28140–28149 (2016).

[31] S. Muramatsu, S. Nakayama, S. N. Kinoshita, Y. Onitsuka, H. Kohguchi, Y. Inokuchi, C. Zhu, and T. Ebata, “Electronic state and photophysics of 2-ethylhexyl-4-methoxycinnamate as uv-b sunscreen under jet-cooled condition,” Journal of Physical Chemistry A **124**, 1272–1278 (2020).

[32] M. Promkatkaew, S. Suramitr, T. M. Karpkird, S. Namuangruk, M. Ehara, and S. Hannongbua, "Absorption and emission spectra of ultraviolet b blocking methoxy substituted cinnamates investigated using the symmetry-adapted cluster configuration interaction method," Journal of Chemical Physics **131**, 224306 (2009).

[33] M. D. Groot, E. V. Gromov, H. Köppel, and W. J. Buma, "High-resolution spectroscopy of methyl 4-hydroxycinnamate and its hydrogen-bonded water complex," Journal of Physical Chemistry B **112**, 4427–4434 (2008).

[34] D. Sampedro, "Computational exploration of natural sunscreens," Physical Chemistry Chemical Physics **13**, 5584–5586 (2011).

[35] M. Promkatkaew, S. Suramitr, T. Karpkird, M. Ehara, and S. Hannongbua, "Absorption and emission properties of various substituted cinnamic acids and cinnamates, based on tddft investigation," **113**, 542–554 (2013).

[36] E. M. M. Tan, S. Amirjalayer, S. Smolarek, A. Vdovin, A. M. Rijs, and W. J. Buma, "Conformational heterogeneity of methyl 4-hydroxycinnamate: A gas-phase uv–ir spectroscopic study," The Journal of Physical Chemistry B **117**, 4798–4805 (2013), pMID: 23574393, https://doi.org/10.1021/jp312624e.

[37] X. P. Chang, C. X. Li, B. B. Xie, and G. Cui, "Photoprotection mechanism of p-methoxy methylcinnamate: A caspt2 study," Journal of Physical Chemistry A **119**, 11488–11497 (2015).

[38] J. Moon, H. Baek, J. S. Lim, and J. Kim, "Tddft and ms-caspt2 study of the excited states of <i>para</i> -methoxymethylcinnamate," Bulletin of the Korean Chemical Society **39**, 427–434 (2018).

[39] C. X. Li, W. W. Guo, B. B. Xie, and G. Cui, "Photodynamics of oxybenzone sunscreen: Nonadiabatic dynamics simulations," Journal of Chemical Physics **145**, 074308 (2016).

[40] K. Yamazaki, Y. Miyazaki, Y. Harabuchi, T. Taketsugu, S. Maeda, Y. Inokuchi, S. N. Kinoshita, M. Sumida, Y. Onitsuka, H. Kohguchi, M. Ehara, and T. Ebata, "Multistep intersystem crossing pathways in cinnamate-based uv-b sunscreens," Journal of Physical Chemistry Letters **7**, 4001–4007 (2016).

[41] X. Zhao, J. Luo, S. Yang, and K. Han, "New insight into the photoprotection mechanism of plant sunscreens: Adiabatic relaxation competing with nonadiabatic relaxation in the cis → trans photoisomerization of methyl sinapate," The Journal of Physical Chemistry Letters **10**, 4197–4202 (2019), pMID: 31287701, https://doi.org/10.1021/acs.jpclett.9b01651.

[42] S. nosuke Kinoshita, Y. Harabuchi, Y. Inokuchi, S. Maeda, M. Ehara, K. Yamazaki, and T. Ebata, "Substitution effect on the nonradiative decay and trans → cis photoisomerization route: a guideline to develop efficient cinnamate based sunscreens," Physical Chemistry Chemical Physics (2020), 10.1039/d0cp04402d.

[43] J. Fan, W. Roeterdink, and W. J. Buma, "Excited-state dynamics of isolated and (micro)solvated methyl sinapate: the bright and shady sides of a natural sunscreen," Molecular Physics **119**, e1825850 (2021).

[44] X.-Y. Xie, C.-X. Li, Q. Fang, and G. Cui, "Mechanistic photochemistry of methyl-4-hydroxycinnamate chromophore and its one-water complexes: Insights from ms-caspt2 study," The Journal of Physical Chemistry A **120**, 6014–6022 (2016), pMID: 27398611, https://doi.org/10.1021/acs.jpca.6b05899.

[45] S. N. Kinoshita, Y. Inokuchi, Y. Onitsuka, H. Kohguchi, N. Akai, T. Shiraogawa, M. Ehara, K. Yamazaki, Y. Harabuchi, S. Maeda, and T. Ebata, "The direct observation of the doorway 1n state of methylcinnamate and hydrogen-bonding effects on the photochemistry of cinnamate-based sunscreens," Physical Chemistry Chemical Physics **21**, 19755–19763 (2019).

[46] X. Zhao, F. Ji, Y. Liang, P. Li, Y. Jia, X. Feng, Y. Sun, Y. Shi, L. Zhu, and G. Zhao, "Theoretical and spectroscopic investigation on ultrafast nonadiabatic photoprotective mechanism of novel ultraviolet protective compounds inspired by natural sunscreens," Journal of Luminescence **223**, 117228 (2020).

[47] M. D. Horbury, A. L. Flourat, S. E. Greenough, F. Allais, and V. G. Stavros, "Investigating isomer specific photoprotection in a model plant sunscreen," Chem. Commun. **54**, 936–939 (2018).

[48] L. F. Alves, R. Gargano, S. K. Alcanfor, L. A. Romeiro, and J. B. Martins, "A chromophoric study of 2-ethylhexyl p-methoxycinnamate," Chemical Physics Letters **516**, 162–165 (2011).

[49] A. Gackowska, M. Przybyłek, W. Studziński, and J. Gaca, "Experimental and theoretical studies on the photodegradation of 2-ethylhexyl 4-methoxycinnamate in the presence of reactive oxygen and chlorine species," Central European Journal of Chemistry **12**, 612–623 (2014).

[50] M. S. Miranda, L. P. da Silva, and J. C. G. E. da Silva, "Uv filter 2-ethylhexyl 4-methoxycinnamate: a structure, energetic and uv-vis spectral analysis based on density functional theory," Journal of Physical Organic Chemistry **27**, 47–56 (2014).

[51] R. D. Garcia, V. G. Maltarollo, K. M. Honório, and G. H. Trossini, "Benchmark studies of uv–vis spectra simulation for cinnamates with uv filter profile," Journal of Molecular Modeling **21**, 1–13 (2015).

[52] R. Car and M. Parrinello, “Unified approach for molecular dynamics and density-functional theory,” Phys. Rev. Lett. **55**, 2471–2474 (1985).

[53] J. P. Perdew, K. Burke, and M. Ernzerhof, “Generalized gradient approximation made simple,” Phys. Rev. Lett. **77**, 3865–3868 (1996).

[54] S. Grimme, “Semiempirical gga-type density functional constructed with a long-range dispersion correction,” Journal of Computational Chemistry **27**, 1787–1799 (2006), https://onlinelibrary.wiley.com/doi/pdf/10.1002/jcc.20495.

[55] C. Møller and M. S. Plesset, “Note on an approximation treatment for many-electron systems,” Physical Review **46**, 618–622 (1934).

[56] T. H. Dunning and P. J. Hay, “Gaussian basis sets for molecular calculations,” Methods of Electronic Structure Theory , 1–27 (1977).

[57] T. H. Dunning, “Gaussian basis sets for use in correlated molecular calculations. i. the atoms boron through neon and hydrogen,” The Journal of Chemical Physics **90**, 1007–1023 (1989).

[58] P. L. Barbieri, P. A. Fantin, and F. E. Jorge, “Gaussian basis sets of triple and quadruple zeta valence quality for correlated wave functions,” Molecular Physics **104**, 2945–2954 (2006).

[59] P. A. Fantin, P. L. Barbieri, A. C. Neto, and F. E. Jorge, “Augmented gaussian basis sets of triple and quadruple zeta valence quality for the atoms h and from li to ar: Applications in hf, mp2, and dft calculations of molecular dipole moment and dipole (hyper)polarizability,” Journal of Molecular Structure: THEOCHEM **810**, 103–111 (2007).

[60] J. Ĉízek, “On the correlation problem in atomic and molecular systems. calculation of wavefunction components in ursell-type expansion using quantum-field theoretical methods,” The Journal of Chemical Physics **45**, 4256–4266 (1966).

[61] J. Čižek and J. Paldus, “Correlation problems in atomic and molecular systems iii. rederivation of the coupled-pair many-electron theory using the traditional quantum chemical methodst,” International Journal of Quantum Chemistry **5**, 359–379 (1971).

[62] G. D. Purvis and R. J. Bartlett, “A full coupled-cluster singles and doubles model: The inclusion of disconnected triples,” The Journal of Chemical Physics **76**, 1910–1918 (1982).

[63] K. Raghavachari, G. W. Trucks, J. A. Pople, and M. Head-Gordon, “A fifth-order perturbation comparison of electron correlation theories,” Chemical Physics Letters **157**, 479–483 (1989).

[64] Y. S. Lee, S. A. Kucharski, and R. J. Bartlett, “A coupled cluster approach with triple excitations,” The Journal of Chemical Physics **81**, 5906–5912 (1984).

[65]"Car-parrinello molecular dynamics cpmd code," Copyright IBM Corp. 1990–2019, MPI für Festkörperforschung Stuttgart, 1997–2001.

[66]T. D. Kühne, M. Iannuzzi, M. D. Ben, V. V. Rybkin, P. Seewald, F. Stein, T. Laino, R. Z. Khaliullin, O. Schütt, F. Schiffmann, D. Golze, J. Wilhelm, S. Chulkov, M. H. Bani-Hashemian, V. Weber, U. Borštnik, M. Taillefumier, A. S. Jakobovits, A. Lazzaro, H. Pabst, T. Müller, R. Schade, M. Guidon, S. Andermatt, N. Holmberg, G. K. Schenter, A. Hehn, A. Bussy, F. Belleflamme, G. Tabacchi, A. Glöß, M. Lass, I. Bethune, C. J. Mundy, C. Plessl, M. Watkins, J. VandeVondele, M. Krack, and J. Hutter, "Cp2k: An electronic structure and molecular dynamics software package -quickstep: Efficient and accurate electronic structure calculations," Journal of Chemical Physics **152**, 194103 (2020).

[67]X. Zhou, T. A. Wesolowski, G. Tabacchi, E. Fois, G. Calzaferri, and A. Devaux, "First-principles simulation of the absorption bands of fluorenone in zeolite l," Phys. Chem. Chem. Phys. **15**, 159–167 (2013).

[68]R. Arletti, E. Fois, L. Gigli, G. Vezzalini, S. Quartieri, and G. Tabacchi, "Irreversible conversion of a water-ethanol solution into an organized two-dimensional network of alternating supramolecular units in a hydrophobic zeolite under pressure," Angewandte Chemie International Edition **56**, 2105–2109 (2017).

[69]G. Tabacchi, "Supramolecular organization in confined nanospaces," ChemPhysChem **19**, 1249–1297 (2018).

[70]E. Fois, G. Tabacchi, and G. Calzaferri, "Orientation and order of xanthene dyes in the one-dimensional channels of zeolite l: Bridging the gap between experimental data and molecular behavior," Journal of Physical Chemistry C **116**, 16784–16799 (2012).

[71]G. Tabacchi, E. Fois, and G. Calzaferri, "Structure of nanochannel entrances in stopcock-functionalized zeolitel composites," Angewandte Chemie International Edition **54**, 11112–11116 (2015), https://onlinelibrary.wiley.com/doi/pdf/10.1002/anie.201504745.

[72]M. J. Frisch, G. W. Trucks, H. B. Schlegel, G. E. Scuseria, M. A. Robb, J. R. Cheeseman, G. Scalmani, V. Barone, B. Mennucci, G. A. Petersson, H. Nakatsuji, M. Caricato, X. Li, H. P. Hratchian, A. F. Izmaylov, J. Bloino, G. Zheng, J. L. Sonnenberg, M. Hada, M. Ehara, K. Toyota, R. Fukuda, J. Hasegawa, M. Ishida, T. Nakajima, Y. Honda, O. Kitao, H. Nakai, T. Vreven, J. A. Montgomery, Jr., J. E. Peralta, F. Ogliaro, M. Bearpark, J. J. Heyd, E. Brothers, K. N. Kudin, V. N. Staroverov, R. Kobayashi, J. Normand, K. Raghavachari, A. Rendell, J. C. Burant, S. S. Iyengar, J. Tomasi, M. Cossi, N. Rega, J. M. Millam, M. Klene, J. E. Knox, J. B. Cross,

V. Bakken, C. Adamo, J. Jaramillo, R. Gomperts, R. E. Stratmann, O. Yazyev, A. J. Austin, R. Cammi, C. Pomelli, J. W. Ochterski, R. L. Martin, K. Morokuma, V. G. Zakrzewski, G. A. Voth, P. Salvador, J. J. Dannenberg, S. Dapprich, A. D. Daniels, Farkas, J. B. Foresman, J. V. Ortiz, J. Cioslowski, and D. J. Fox, "Gaussian09 Revision E.01," Gaussian Inc. Wallingford CT 2009.

[73] M. Valiev, E. J. Bylaska, N. Govind, K. Kowalski, T. P. Straatsma, H. J. V. Dam, D. Wang, J. Nieplocha, E. Apra, T. L. Windus, and W. A. D. Jong, "Nwchem: A comprehensive and scalable open-source solution for large scale molecular simulations," Computer Physics Communications **181**, 1477–1489 (2010).

[74] E. Aprà, E. J. Bylaska, W. A. D. Jong, N. Govind, K. Kowalski, T. P. Straatsma, M. Valiev, H. J. V. Dam, Y. Alexeev, J. Anchell, V. Anisimov, F. W. Aquino, R. Atta-Fynn, J. Autschbach, N. P. Bauman, J. C. Becca, D. E. Bernholdt, K. Bhaskaran-Nair, S. Bogatko, P. Borowski, J. Boschen, J. Brabec, A. Bruner, E. Cauët, Y. Chen, G. N. Chuev, C. J. Cramer, J. Daily, M. J. Deegan, T. H. Dunning, M. Dupuis, K. G. Dyall, G. I. Fann, S. A. Fischer, A. Fonari, H. Früchtl, L. Gagliardi, J. Garza, N. Gawande, S. Ghosh, K. Glaesemann, A. W. Götz, J. Hammond, V. Helms, E. D. Hermes, K. Hirao, S. Hirata, M. Jacquelin, L. Jensen, B. G. Johnson, H. Jónsson, R. A. Kendall, M. Klemm, R. Kobayashi, V. Konkov, S. Krishnamoorthy, M. Krishnan, Z. Lin, R. D. Lins, R. J. Littlefield, A. J. Logsdail, K. Lopata, W. Ma, A. V. Marenich, J. M. D. Campo, D. Mejia-Rodriguez, J. E. Moore, J. M. Mullin, T. Nakajima, D. R. Nascimento, J. A. Nichols, P. J. Nichols, J. Nieplocha, A. Otero-De-La-Roza, B. Palmer, A. Panyala, T. Pirojsirikul, B. Peng, R. Peverati, J. Pittner, L. Pollack, R. M. Richard, P. Sadayappan, G. C. Schatz, W. A. Shelton, D. W. Silverstein, D. M. Smith, T. A. Soares, D. Song, M. Swart, H. L. Taylor, G. S. Thomas, V. Tipparaju, D. G. Truhlar, K. Tsemekhman, T. V. Voorhis, A. Vázquez-Mayagoitia, P. Verma, O. Villa, A. Vishnu, K. D. Vogiatzis, D. Wang, J. H. Weare, M. J. Williamson, T. L. Windus, K. Woliński, A. T. Wong, Q. Wu, C. Yang, Q. Yu, M. Zacharias, Z. Zhang, Y. Zhao, and R. J. Harrison, "Nwchem: Past, present, and future," Journal of Chemical Physics **152**, 184102 (2020).

[75] B. P. Pritchard, D. Altarawy, B. Didier, T. D. Gibson, and T. L. Windus, "New basis set exchange: An open, up-to-date resource for the molecular sciences community," Journal of Chemical Information and Modeling **59**, 4814–4820 (2019).

[76] V. Arjunan, R. Anitha, S. Thenmozhi, M. K. Marchewka, and S. Mohan, "Potential energy profile, structural, vibrational and reactivity descriptors of trans-2-methoxycinnamic acid by ftir,

ft-raman and quantum chemical studies," Journal of Molecular Structure **1113**, 42–54 (2016).

[77] L. Gigli, R. Arletti, G. Tabacchi, M. Fabbiani, J. G. Vitillo, G. Martra, A. Devaux, I. Miletto, S. Quartieri, G. Calzaferri, and E. Fois, "Structure and host–guest interactions of perylene–diimide dyes in zeolite l nanochannels," The Journal of Physical Chemistry C **122**, 3401–3418 (2018).

[78] L. Gigli, R. Arletti, G. Tabacchi, E. Fois, J. G. Vitillo, G. Martra, G. Agostini, S. Quartieri, and G. Vezzalini, "Close-packed dye molecules in zeolite channels self-assemble into supramolecular nanoladders," The Journal of Physical Chemistry C **118**, 15732–15743 (2014).

TABLE I. Zpe and zpe-corrected MP2 energies (Hartree) and relative energies ΔE (kcal/mol) of the four conformers with different basis sets.

Basis set[a]	Cis1	Trans1	Cis2	Trans2
zpe-mp2/cc-pvdz+S	0.410052	0.409026	0.409977	0.409137
cc-pvdz+S	-924.040302	-924.039870	-924.041949	-924.042305
ΔE	1.257	1.528	0.223	0.000
dzp++	-924.144505	-924.141180	-924.145834	-924.143490
ΔE	-0.637	1.449	-1.471	0.000
aug-cc-pvdz	-924.197677	-924.193647	-924.198970	-924.196188
ΔE	-0.934	1.595	-1.746	0.000
aug-cc-pvtz	-925.008744	-925.010046	-925.010656	-925.013037
ΔE	2.694	1.877	1.494	0.000
tzp	-924.924976	-924.927379	-924.926980	-924.930495
ΔE	3.464	1.955	2.206	0.000
tzp++	-925.000783	-925.001053	-925.002618	-925.004079
ΔE	2.068	1.899	0.917	0.000
tzp++ (Full Core)	-925.430020	-925.428168	-925.431526	-925.431100
ΔE	0.678	1.840	-0.267	0.000
HF/cc-pvdz+S	-920.995261	-921.014042	-920.999511	-921.016629
ΔE	13.408	1.623	10.741	0.000
HF/tzp++	-921.229814	-921.251164	-921.234532	-921.253758
ΔE	15.025	1.628	12.065	0.000

[a] Zpe-corrections and geometries were obtained by optimizing all conformers at the MP2/cc-pvdz+S level. The last four lines refer to HF calculations on the same geometries. ΔEs are relative to the Trans2 energies.

TABLE II. ZPE-corrected Coupled Cluster energies (Hartree) and relative energies ΔE (kcal/mol) of the four conformers with different basis sets.

Basis set[a]	Cis1	Trans1	Cis2	Trans2
CCSD/cc-pvdz+S	-924.203270	-924.207112	-924.205486	-924.209219
ΔE	3.733	1.322	2.342	0.000
CCSD(t)/cc-pvdz+S	-924.326933	-924.328537	-924.328767	-924.330864
ΔE	2.466	1.460	1.316	0.000
CCSD+T(CCSD)/cc-pvdz+S	-924.331918	-924.333471	-924.333756	-924.335955
ΔE	2.533	1.559	1.380	0.000
CCSD/dzp++	-924.302624	-924.303659	-924.304522	-924.305618
ΔE	1.879	1.230	0.688	0.000
CCSD(t)/dzp++	-924.424804	-924.423100	-924.426275	-924.425232
ΔE	0.269	1.338	-0.654	0.000
CCSD+T(CCSD)/dzp++	-924.430358	-924.428582	-924.431827	-924.430874
ΔE	0.324	1.438	-0.598	0.000

[a] ZPE corrections and geometries were obtained by optimizing all conformers at the MP2/cc-pvdz+S level. ΔEs are relative to the Trans2 energies.

TABLE III. Moments of Inertia (a.u.)

Cis1	7377.9281	4871.3189	9168.6493
Trans1	15941.9319	4225.6962	16912.0170
Cis2	7629.6061	4904.8131	10007.9806
Trans2	17820.7804	3793.3202	20231.0798